Selective Reduction of Radiotracer Trapping by Deuterium Substitution: Comparison of Carbon-11-L-Deprenyl and Carbon-11-Deprenyl-D2 for MAO B Mapping

Joanna S. Fowler, Gene-Jack Wang, Jean Logan, Shan Xie, Nora D. Volkow, Robert R. MacGregor, David J. Schlyer, Naomi Pappas, David L. Alexoff, Clifford Patlak and Alfred P. Wolf

Chemistry and Medical Departments, Brookhaven National Laboratory, Upton, New York; and Departments of Psychiatry and Surgery, University Hospital, State University of New York, Stony Brook, New York

Recent human PET studies with the monoamine oxidase B (MAO B) tracer [^{11}C]L-deprenyl show that the rapid rate of radiotracer trapping relative to transport reduces the sensitivity of the tracer in regions of high MAO B concentration. This study investigates the use of deuterium substituted L-deprenyl ([^{11}C]L-deprenyl-D2) to reduce the rate of trapping in tissue and to improve sensitivity. **Methods:** Five normal subjects (43–64 yr) were studied with [^{11}C]L-deprenyl and [^{11}C]L-deprenyl-D2 on the same day. Time-activity data from different brain regions and the arterial plasma were analyzed using a three-compartment model as well as graphical analysis for irreversible systems. **Results:** For both tracers, maximum radioactivity accumulation occurred at about 5 min. For [^{11}C]L-deprenyl, ^{11}C concentration peaked at 5 min and remained constant throughout the study. With [^{11}C]L-deprenyl-D2, peak ^{11}C concentration also occurred at about 5 min but was followed by an initial washout. Carbon-11 concentration generally plateaued from 30 to 60 min. The plateau for [^{11}C]L-deprenyl was higher than the plateau for [^{11}C]L-deprenyl-D2. Data analysis by a three-compartment model and by graphical analysis showed that deuterium substitution: (a) does not affect plasma to tissue transport (K_1); (b) reduces the rate of trapping of ^{11}C in all brain regions; (c) facilitates the separation of model terms related to radiotracer delivery from radiotracer trapping in tissue; and (d) improves tracer sensitivity. **Conclusion:** This study demonstrates that deuterium substitution causes a significant reduction in the rate of trapping of labeled deprenyl, providing a direct link between radiotracer uptake and MAO B in the human brain and enhancing tracer sensitivity to changes in MAO B concentration.

Key Words: monoamine oxidase B; carbon-11-deprenyl-D2; enzyme mapping

J Nucl Med 1995; 36:1255–1262

Monoamine oxidase is a flavin-containing enzyme located in the outer mitochondrial membrane. It catalyzes the oxidation of amines from endogenous as well as exogenous sources. It exists in subtypes MAO A and MAO B, which are distinguished by different amino acid sequences and different substrate and inhibitor profiles (*1*). In the human brain, MAO B predominates (B:A = 4:1) and is associated mainly with glial cells (*2*). Unlike most enzymes and neurotransmitter receptors and transporters, MAO B *increases* with normal aging and in neurodegenerative diseases (*3–6*). This increase has been attributed to an increase in glial cells in response to age-related or disease-associated neuron loss and gliosis (*7,8*).

Carbon-11-L-deprenyl is a selective irreversible inhibitor of MAO B which labels functionally active enzyme (*9*). The design concept is based on "suicide" enzyme inactivation in which the MAO B catalyzed oxidation of labeled deprenyl within the enzyme substrate complex results in the cleavage of a carbon-hydrogen bond leading to an activated intermediate which covalently labels the enzyme. Thus, the PET image after the injection of labeled deprenyl represents the distribution of functional MAO B activity. Prior studies have demonstrated that labeled L-deprenyl shows appropriate regional distribution, stereoselectivity and pharmacology to support its use to map brain MAO B in vivo (*9*). In addition, mechanistic studies with [^{11}C]L-deprenyl-D2 showed that it is the MAO B catalyzed cleavage of the C-H bond of the propargyl group of L-deprenyl which contributes to the trapping of tracer in tissue (*10*).

We and others have used [^{11}C]L-deprenyl in pharmacodynamic studies of the MAO B inhibitor drugs Ro 19 6327 (*11,12*) and L-deprenyl (*13,14*) and to measure the rate of synthesis of MAO B in the baboon brain (*15*) and in the human brain (*13*) and to map the enzyme in different disease states (*16*). We found, however, in some human studies that in regions of high MAO (basal ganglia and thalamus) the tracer is trapped at a rate which is similar to or exceeds the rate at which it is delivered by the plasma (*11*). This limits tracer uptake and leads to an underestimation of

Received Sep. 6, 1994; revision accepted Dec. 27, 1994.
For correspondence or reprints contact: Joanna S. Fowler, MD, Chemistry Department, Brookhaven National Laboratory, Upton, NY 11973-5000.

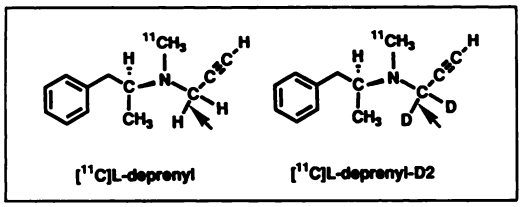

FIGURE 1. Structures of [^{11}C]L-deprenyl and [^{11}C]L-deprenyl-D2. The arrows indicate the carbon-hydrogen and carbon-deuterium bonds which are cleaved during enzyme catalyzed oxidation.

MAO B in these regions so that changes in regional radioactivity are less sensitive to changes in MAO B concentration and more sensitive to changes in delivery. This results in a flow-limited image (*17*). Though this is not a problem when labeled L-deprenyl is used in studies of MAO B inhibitor drugs or of MAO B synthesis where MAO B is totally or partially inhibited, it is a serious limitation in regions of high MAO B, especially in cases where blood flow is low.

We have investigated the use of deuterium-substituted L-deprenyl ([^{11}C]L-deprenyl-D2) to reduce the rate of radiotracer trapping in the human brain and to improve sensitivity as a strategy for developing a *positive* tracer (e.g., a tracer whose uptake would increase rather than decrease as neurons are lost and as glial cells proliferate) in neurodegenerative disease. We examined the use of [^{11}C]L-deprenyl-D2 in order to maintain the original radiotracer design concept but at the same time to *selectively* reduce the rate of trapping in tissue based on previous studies in baboons (*10*). We report here on PET studies in five normal human subjects comparing [^{11}C]L-deprenyl and [^{11}C]L-deprenyl-D2 (Fig. 1). Time-activity data from brain regions and from arterial plasma were analyzed using a three-compartment model and graphical analysis for irreversible systems (*18–21*).

MATERIALS AND METHODS

Subjects

Five normal subjects consisting of (4 men, 1 woman), aged 43–64 yr were recruited for this study. The subjects were nonsmokers and free of neurologic, psychiatric and cardiovascular disease. Subjects were free of medication. The studies followed the guidelines of the Human Subjects Research Committee at Brookhaven National Laboratory.

PET

Scans were obtained on a whole-body, high-resolution positron emission tomograph (6 × 6 × 6.5 mm, FWHM, 15 slices, Computer Technologies Inc., CTI 931, Knoxville, TN). To ensure accurate repositioning of subjects in the PET scanner for the repeated scans, an individually molded headholder was made for each subject. The head of the subject was then positioned in the gantry with the aid of three orthogonal laser lines, two of which were placed parallel to the left and right canthomeatal lines and one parallel to the sagittal plane. This strategy allows an accuracy of repositioning within 2 mm (*22*). A transmission scan was obtained with a ^{68}Ge ring source before the emission scan to correct for attenuation. Catheters were placed in an antecubital vein for tracer injection and in the radial artery for blood sampling.

Tracers

Carbon-11-L-deprenyl and [^{11}C]L-deprenyl-D2 were prepared as described previously (*10,23*). Each subject received both tracers with a time interval of 2–3 hr between injections. Two subjects had [^{11}C]L-deprenyl first and three of the subjects had [^{11}C]L-deprenyl-D2 first. The dose of [^{11}C]L-deprenyl or [^{11}C]deprenyl-D2 ranged from 5 to 8.5 mCi (6–29 μg). Sequential PET scans were obtained immediately after injection for a total of 60 min with the following timing: 10 × 1 min frames; 4 × 5 min frames; 3 × 10 min frames. One subject was scanned twice with [^{11}C]L-deprenyl-D2: at baseline and 1 wk later after being treated with L-deprenyl (10 mg/day) for 1 wk to inhibit MAO B.

Plasma Analysis

During the PET scan, arterial blood samples were withdrawn every 2.5 sec for the first 2 min (Ole Dich automatic blood sampler, Hvidovre, Denmark), then every minute from 2 to 6 min, then at 8, 10, 15, 20, 30, 45 and 60 min. The tubing for sampling whole blood from the automated blood sampling instrument was washed with a diluted solution of L-deprenyl prior to blood collection to prevent radioactivity sticking. Each arterial blood sample was centrifuged and plasma pipetted and counted. Duplicate plasma samples at 1, 5, 10, 30 and 60 min were analyzed for [^{11}C]L-deprenyl (or [^{11}C]L-deprenyl-D2) using a solid phase extraction. Plasma (0.050–0.4 ml) was added to water (3 ml) and the mixture was added to 2 ml of water and applied to a Bond Elut (Varian) LRC C-18 solid phase extraction cartridge (0.5 g). The mixture was slowly pushed through the cartridge. An additional 5 ml of water was applied and eluted, followed by 6–7 ml of methanol. The total sample, each fraction and the column were counted. Carbon-11-L-deprenyl eluted primarily with the methanol. Control studies with [^{11}C]L-deprenyl in plasma confirmed the elution pattern. On some of the samples, an HPLC analysis of the methanol fraction [ODS 2; 5 μ; methanol-to-ammonium formate (0.05 *M*) (65:35)] showed that the radioactivity was >95% L-deprenyl. Independent HPLC analysis of selected plasma samples gave the same value for unchanged tracer as the solid-phase analysis. For the 1-, 5- and 10-min plasma samples, less than 5% of the total radioactivity remained on the cartridge. However, the cartridge frequently retained 10%–15% of the radioactivity for the 30-min sample. This may be [^{11}C]methamphetamine which has been shown to be retained completely (>98%) on the column using this elution procedure (unpublished observations).

ROI Determination

Regions of interest (ROIs) were drawn directly on PET scans. For the purpose of region identification, we added the images obtained from 30 to 60 min after tracer injection. A template that used the brain atlas of Matsui and Hirano as a reference (*24*) was projected into the averaged PET image and manually fitted for an appropriate neuroanatomical location. The regions were then projected to the dynamic scans. ROIs for the following brain areas were obtained: occipital cortex, cingulate gyrus, thalamus, basal ganglia and cerebellum. Regions were identified in at least two contiguous slices and the weighted average was obtained for each region. In addition, an approximate measure for the whole brain (global) was obtained by averaging radioactivity concentrations in the six central slices.

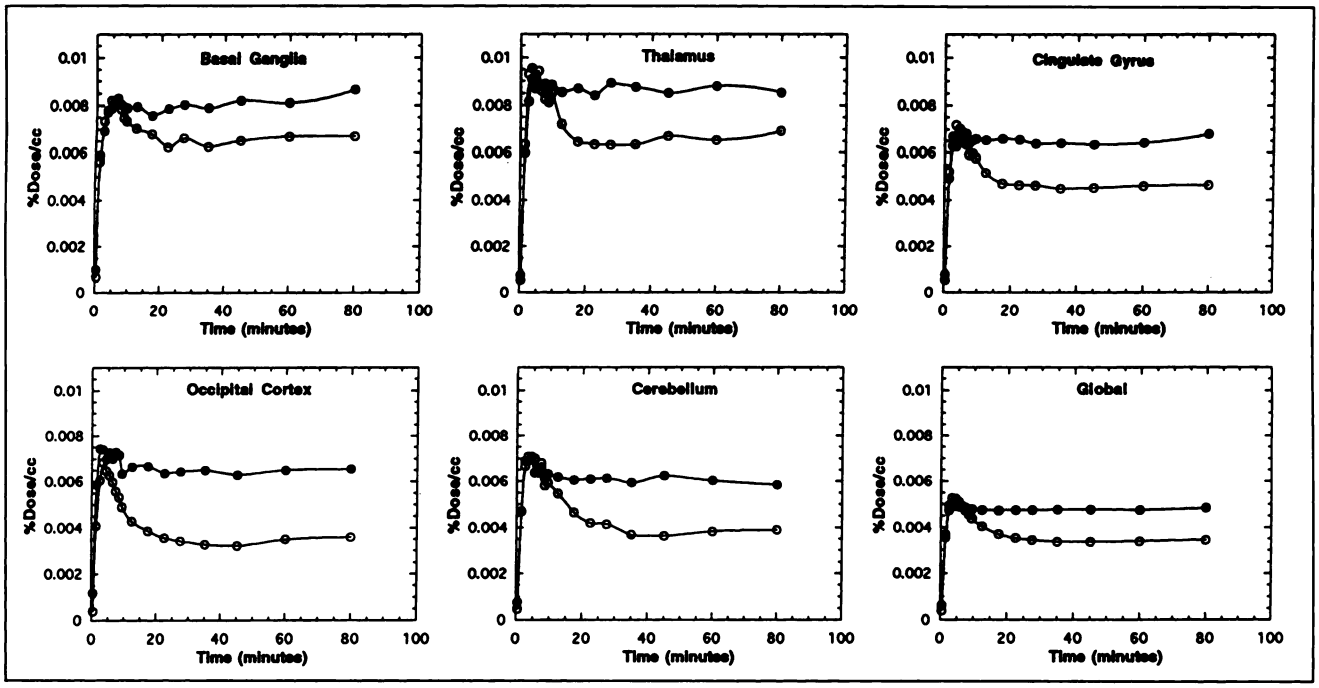

FIGURE 2. Time-activity curves for five brain regions and for the global region for [^{11}C]L-deprenyl (closed circles) and [^{11}C]L-deprenyl-D2 (open circles) for one of the subjects (male, 43 yr). Peak uptake is similar in time and magnitude for the two tracers but with [^{11}C]L-deprenyl, ^{11}C in brain plateaus at peak value while with [^{11}C]L-deprenyl-D2, the plateau follows an initial clearance after the peak.

Data Analysis

Time-activity data from PET and the arterial plasma were analyzed using a three-compartment model and graphical analysis for irreversible systems (*19*). An approximate blood volume correction (4%) was subtracted from the PET data prior to parameter optimization. These analyses strategies have been applied previously to [^{11}C]L-deprenyl kinetics in both human (*11,13*), and baboon brain (*10,15*). In the graphical analysis for irreversible systems, the slopes (K_i) were taken as an average of slopes between 6 and 45 min and 6 and 55 min.

The model equations of the three-compartment model were solved numerically (*25*). Optimum values for the model parameters were determined by the Levenberg-Marquardt method (*26*). The three model parameters optimized were K_1 (the plasma-to-tissue transfer constant); k_2 (the tissue-to-plasma transfer constant); and k'_3E (the term determining the rate of trapping in tissue which is proportional to the amount of enzyme present (*10,11*). The parameters are reported as K_1, λ (equal to K_1/k_2) and $\lambda k'_3E$ since this appears to be a better measure of relative enzyme concentration than k'_3E.

Sensitivity

The enzyme concentration is the quantity of primary interest but since it is not determined directly but inferred from the model parameters (Ki and $\lambda k'_3E$), the accuracy with which these parameters reflect the enzyme concentration is related to their sensitivity to variations in enzyme concentration. This can be assessed in terms of the normalized derivative which for Ki is $\delta K_i/\delta \lambda k'_3E \times \lambda k'_3E/K_i$ and is given by (*27*):

$$1 - \frac{\lambda k'_3E}{K_1 + \lambda k'_3E},$$

where $K_1 >> \lambda k'_3E$, Ki is approximately 1 which means that any change in enzyme parameter $\lambda k'_3E$ is directly proportional to a change in the signal (Ki). Similarly, for the model fit, the normalized derivative is given by $dS/dk'_3E \times k'_3E/S$ where S is the predicted radioactivity uptake determined from the model solution (*17*).

RESULTS

The concentration of ^{11}C peaked at about 5 min for both [^{11}C]L-deprenyl and [^{11}C]L-deprenyl-D2. With [^{11}C]L-deprenyl, the ^{11}C concentration plateaued at peak uptake. With [^{11}C]L-deprenyl-D2, peak ^{11}C concentration also occurred at about 5 min but was followed by a washout and plateau from 30 to 60 min (see Fig. 2) for two tracers in five brain regions of one subject (thalamus, basal ganglia, cingulate gyrus, occipital cortex and cerebellum) and for the global region). The average plateau uptake for [^{11}C]L-deprenyl was higher than the average plateau for [^{11}C]L-deprenyl-D2 for the different brain regions (Fig. 3). The highest uptake for both tracers is in the basal ganglia, thalamus and cingulate gyrus.

The total ^{11}C in plasma samples was greater in all cases for [^{11}C]L-deprenyl-D2 than for [^{11}C]L-deprenyl. The percentage of parent tracer in plasma at 1, 5, 10, 30 and 60 min, however, was not significantly different for the two tracers ($p > 0.15$, paired t-test and two-tail). Average values for [^{11}C]L-deprenyl and [^{11}C]L-deprenyl-D2 for the percent of total ^{11}C as a parent tracer were 97.5 ± 2.4, 84.2 ± 3.2, 70 ± 4.6, 35.8 ± 6.6, 15.9 ± 4.2 at 1, 5, 10, 30 and 60 min, respectively. The value of the integral of the tracer's arterial plasma concentration was greater (average of 1.27 ± 0.13 times greater over 60 min) for [^{11}C]L-deprenyl-D2 than for [^{11}C]L-deprenyl in all subjects. Figure 4A

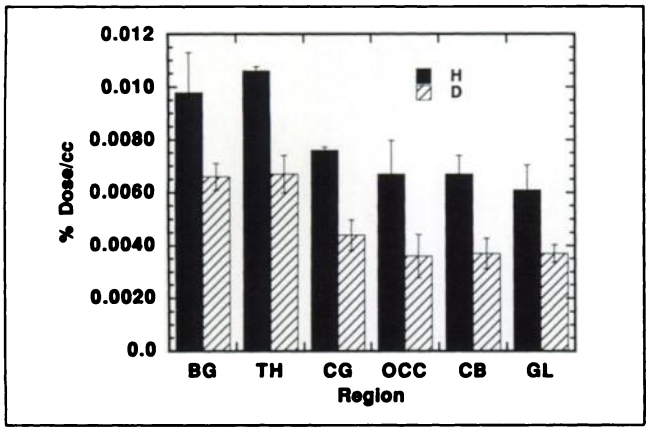

FIGURE 3. Bar graph depicting mean ± s.d. for the uptake in different brain regions and the global region for the five subjects for [^{11}C]L-deprenyl (H) and [^{11}C]L-deprenyl-D2 (D). Abbreviations: BG (basal ganglia); TH (thalamus); CG (cingulate gyrus); OCC (occipital cortex); CB (cerebellum); GL (global).

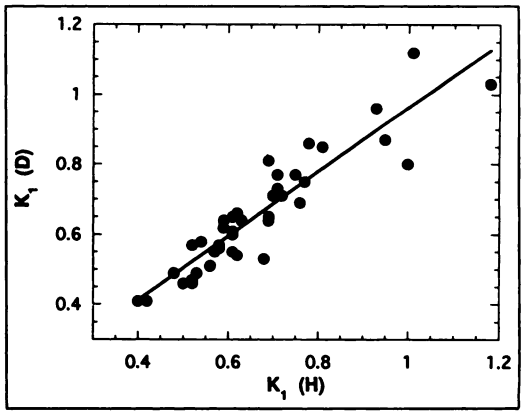

FIGURE 5. Plot showing the correlation of the blood to brain transfer constants (K_1) for [^{11}C]L-deprenyl (H) and [^{11}C]L-deprenyl-D2 (D) for all brain regions for all of the subjects ($r = 0.900$; $p = 0.0001$; slope = 0.94).

shows a plasma time-activity curve for the two tracers and Figure 4B shows the integral of the time-activity curve over 60 min.

Values for K_1, the plasma to brain transport constant, were estimated from a three-compartment model and ranged from 0.39 to 1.12 for the two tracers. They were highly correlated ($r = 0.92$; $p < 0.0001$; slope = 0.92) as shown in Figure 5. Graphical analysis gave linear plots for times greater than 6 min for both tracers (Fig. 6 for graphical analysis for thalamus and cerebellum for the two tracers) illustrating irreversible trapping in brain over the course of the study. Mean values for the model terms estimated from a three-compartment model and the model terms from graphical analysis are shown in Tables 1 and 2. Values for $\lambda k'_3 E$ and for K_i were greater for [^{11}C]L-deprenyl than for [^{11}C]L-deprenyl-D2. MAO B inhibition by L-deprenyl in one of the subjects reduced Ki by 90%, 93% and 78% for the basal ganglia, thalamus and global regions, respectively.

A sensitivity analysis was performed for the model terms related to the trapping of tracer in tissue (*17*). There was an approximate twofold increase in sensitivity with [^{11}C]L-deprenyl-D2 relative to [^{11}C]L-deprenyl. An examination of these values in Tables 2 and 3 show that sensitivity is lowest for the basal ganglia and the thalamus which are regions known to have the highest levels of MAO B. Additionally, an examination of the sensitivity as a function of fractional changes in the model term proportional to enzyme concentration ($\lambda k'_3 E$) showed that this fall-off in sensitivity with increasing values of $\lambda k'_3 E$ is far more pronounced for [^{11}C]L-deprenyl than for [^{11}C]L-deprenyl-D2 (Fig. 7).

DISCUSSION

Deuterium substitution is frequently applied in mechanistic studies in the study of organic and biochemical reactions (*28*). It is based on the principle that carbon-deuterium bonds are stronger than carbon-hydrogen bonds. Thus if a particular carbon-hydrogen bond is cleaved in the rate-limiting (or rate-contributing) step in a chemical reaction, then deuterium substitution should reduce the reaction rate. The traditional value of deuterium isotope studies has been in mechanistic studies to identify the specific carbon-hydrogen bond which is cleaved in the rate limiting step in a chemical or biochemical transformation. Deuterium isotope effects have been valuable mechanistic tools in the study of MAO catalyzed oxidation of amines beginning with the classical studies of Belleau and Moran in 1960 (*29*). This mechanistic tool has also been used with a num-

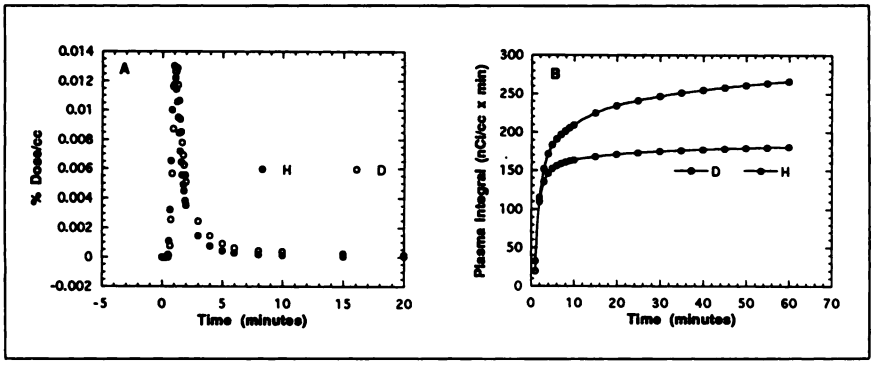

FIGURE 4. (A) The first 20 min of the time-activity curves for plasma for the two tracers in which the concentration for [^{11}C]L-deprenyl-D2 is higher. This is more obvious in (B) which shows the plasma integral over 60 min.

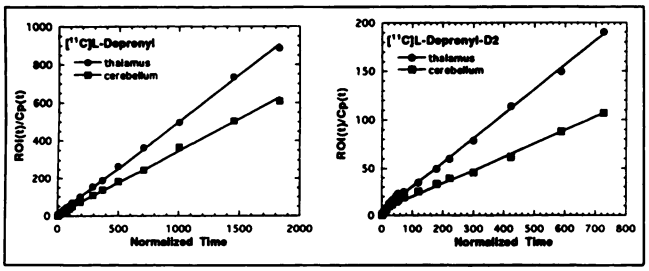

FIGURE 6. Graphical analysis of [^{11}C]L-deprenyl and [^{11}C]L-deprenyl-D2 time-activity data from the thalamus and cerebellum for a 43-yr-old man. The two plots have different y-scales. Slopes are 0.49 and 0.33 min^{-1}, respectively for the thalamus and cerebellum for [^{11}C]L-deprenyl and 0.25 and 0.14 min^{-1} for the thalamus and cerebellum for [^{11}C]L-deprenyl-D2. The ratios of the slopes are 1.78 and 1.48, respectively, reflecting the greater dynamic range for [^{11}C]L-deprenyl-D2.

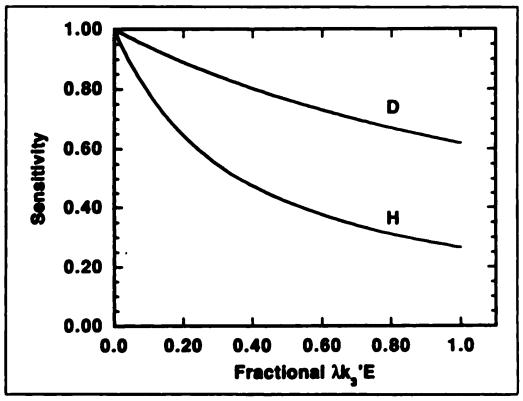

FIGURE 7. Plot showing the changes in sensitivity (see Methods for a definition) of [^{11}C]L-deprenyl (H) and [^{11}C]L-deprenyl-D2 (D) with increasing fractional values of $\lambda k'_3E$. Sensitivity drops off at a far faster rate with H than with D as the $\lambda k'_3E$ values increase.

ber of positron emitter-labeled tracers for MAO in studies in small animals (*30,31*). We have used deuterium substitution in labeled deprenyl with PET to determine that cleavage of the carbon-hydrogen bond alpha to the amino group in the propargyl function of L-deprenyl contributes to the irreversible trapping of ^{11}C in baboon brain (*10*). Though this study was mechanistic in nature, it also suggested that this approach could be used to selectively reduce the rate of trapping in tissue and formed the basis for the present study.

In the case of labeled deprenyl, it is the kinetic term related to the trapping of ^{11}C in the brain which is associated with the concentration of MAO B and which is specifically of interest for PET studies. However, the difficulty in separating kinetic terms related to radiotracer trapping from terms related to radiotracer delivery has limited the sensitivity of [^{11}C]L-deprenyl in regions of high MAO B concentration. To illustrate this problem, consider the simplified equation depicting the model for the trapping of labeled L-deprenyl in the brain:

$$S_p \underset{k_2}{\overset{K_1}{\rightleftharpoons}} S_b + E \xrightarrow{k'_3} S_{tr},$$

PET ROI

where S_p is tracer in plasma; S_b is tracer in brain not bound to enzyme; E is enzyme concentration (considered to remain constant during the course of the PET experiment); and S_{tr} is trapped tracer (i.e., "labeled" MAO B). The term k'_3E determines the rate of trapping of tracer in tissue. When $k'_3E \gg k_2$ the trapping of tracer is determined primarily by K_1 as illustrated below:
Therefore, when $k'_3E \gg k_2$

$$\frac{dS_{tr}}{dt} = K_1 S_p,$$

while the desirable situation is to have $k_2 \gg k'_3E$ giving

$$\frac{dS_{tr}}{dt} = \lambda k'_3 E S_p$$

TABLE 1
Means and Coefficients of Variation for Different Brain Regions for Model Terms Calculated from a Three-Compartment Model for [^{11}C]L-deprenyl (H) and [^{11}C]L-deprenyl-D2 (D)*

Region	K_1(H)	K_1(D)	λ(H)	λ(D)	$\lambda k'_3E$(H)	$\lambda k'_3E$(D)	Sensitivity (H)	Sensitivity (D)
Global	0.49 (16%)	0.50 (19%)	4.33 (26%)	3.5 (11%)	0.78 (29%)	0.18 (22%)	0.4 (29%)	0.69 (6%)
Cerebellum	0.65 (26%)	0.63 (19%)	5.3 (20%)	4.7 (5%)	0.77 (36%)	0.16 (30%)	0.45 (37%)	0.70 (4%)
Occipital cortex	0.81 (33%)	0.69 (33%)	3.77 (41%)	3.75 (17%)	0.77 (40%)	0.16 (44%)	0.48 (45%)	0.73 (3%)
Cingulate gyrus	0.65 (15%)	0.65 (20%)	4.75 (41%)	3.55 (15%)	0.93 (34%)	0.21 (28%)	0.42 (28%)	0.72 (7%)
Basal ganglia	0.71 (20%)	0.73 (22%)	8.08 (45%)	5.12 (18%)	1.64 (33%)	0.37 (27%)	0.32 (38%)	0.64 (12%)
Thalamus	0.81 (15%)	0.85 (21%)	15.9 (97%)	5.59 (9%)	1.60 (33%)	0.35 (26%)	0.31 (44%)	0.68 (9%)

*Data from the five subjects who received both tracers on the same day.

K_1 (units: ml/min/ml) is the blood-to-brain transport constant; λ (units: cc(tissue)/ml (plasma)) is the ratio K_1/k_2; and $\lambda k'_3E$ (units: cc(tissue)(ml(plasma))$^{-1}$ min^{-1}E) is proportional to MAO B concentration. Sensitivity is defined as $dS/dk'_3E(k'_3E/S)$ where S is equal to the tracer uptake.

TABLE 2
Means and Coefficients of Variation for the Influx Constants (K_i(cc(tissue) (ml(plasma)$^{-1}$ min^{-1})) Determined by Graphical Analysis for [^{11}C]L-deprenyl and [^{11}C]L-deprenyl-D2.

Region	K_i(H)	K_i(D)	Sensitivity (H)	Sensitivity (D)
Global	0.28 (17%)	0.12 (16%)	0.40 (30%)	0.74 (9%)
Cerebellum	0.31 (15%)	0.11 (24%)	0.49 (31%)	0.80 (9%)
Occipital cortex	0.32 (27%)	0.12 (40%)	0.56 (30%)	0.82 (10%)
Cingulate gyrus	0.35 (19%)	0.15 (24%)	0.44 (23%)	0.76 (9%)
Basal ganglia	0.46 (10%)	0.23 (19%)	0.35 (35%)	0.67 (14%)
Thalamus	0.49 (8%)	0.23 (20%)	0.39 (28%)	0.72 (11%)

Sensitivity is defined as $dK_i/d\lambda k'_3E(\lambda k'_3E/K_i)$.

when the nonbound tracer has reached steady state ($dS_b/dt \approx 0$). The equation for nonbound tracer is:

$$\frac{dS_b}{dt} = K_1S_p - (k'_3E + k_2)S_b$$

which in the steady state reduces to:

$$S_b = \frac{K_1S_p}{(k_2 + k'_3E)},$$

so that

$$\frac{dS_{tr}}{dt} = k'_3ES_b = \frac{K_1k'_3E}{(k_2 + k'_3E)} S_p.$$

Under the first condition ($k'_3E >> k_2$), changes in S_{tr} are not related to changes in MAO B but to changes in delivery (K_1) while under the second condition ($k_2 >> k'_3E$), changes in S_{tr} are directly related to changes in MAO B concentration (E).

The effects of blood flow occur through the parameters K_1 and k_2. Due to the high extraction of L-deprenyl, K_1 is dominated by flow rather than capillary permeability and therefore decreases in blood flow can decrease sensitivity to changes in MAO B. In the baboon, previous studies showed that K_1 and k_2 are considerably larger than k'_3E which is the optimal condition for sensitivity. In humans, however, K_1 and k_2 are smaller than in the baboon (*10*) and k'_3E is large in regions such as the thalamus and basal ganglia (see reference *11*, Table 2).

The kinetic term k'_3E can be reduced by depleting the enzyme concentration (E) (which can be accomplished by treatment with MAO B inhibitor drugs) or by reducing the rate constant (k'_3). Either of these would be predicted to increase the sensitivity of S_{tr} to changes in enzyme concentration and decrease the sensitivity to changes in blood flow. Since MAO catalyzed oxidation is known to involve cleavage of a carbon-hydrogen bond in the rate-limiting step (Fig. 1), the use of deuterium substitution provides the opportunity to selectively reduce the rate of trapping. Moreover, unlike the use of pharmacological challenge which may have multiple effects in a living system, the deuterium isotope effect would be predicted to operate only on the enzymatic cleavage.

In this study, model parameters have been reported as λ and $\lambda k'_3E$ because the combination $\lambda k'_3E$ was found to reflect the regional enzyme concentration more accurately than k'_3E alone. We have previously found that the combination parameter was more stable under test-retest conditions for the dopamine D2 receptor ligand [^{18}F]N-methylspiroperidol for which the same three-compartment model was used (*27*). The need to use $\lambda k'_3E$ rather than k'_3E may reflect the possibility that the three-compartment model is an oversimplification of the actual enzyme inactivation which is a multistep process with the formation of intermediate species prior to bond cleavage that inactivates the enzyme (*32*).

K_1 was not changed by deuterium substitution which was predicted since isotopic substitution should have minimal effects on the parameters which affect tracer delivery. In contrast, deuterium substitution greatly reduced radiotracer uptake in tissue as well as the model terms (K_i and $\lambda k'_3E$) related to radiotracer trapping in tissue (Tables 1 and 2). This directly links the cleavage of this particular carbon-hydrogen bond to the trapping of tracer in tissue. Since this is the bond known to be cleaved in the MAO-catalyzed oxidation of amines, we have direct evidence that the regional distribution of the tracer is associated with the regional distribution of MAO B.

In assessing the value of a particular tracer for measuring the regional concentration of biological substrates like enzymes or neurotransmitter receptors or transporters, it is important to compare model terms to postmortem values for the biological substrate. Since no single postmortem study provides MAO B levels for all of the regions chosen in this PET study, we compared the ratio of regional values for K_i for [^{11}C]L-deprenyl and [^{11}C]L-deprenyl-D2 to the same ratios of the measured values of MAO B in the postmortem human brain from the literature (*33–35*). There is a good correlation between MAO B concentration ratios and K_i ratios for both tracers. The range of values is, however, greater for [^{11}C]L-deprenyl-D2 than for [^{11}C]L-deprenyl in accordance with postmortem data (Fig. 8).

CONCLUSION

We have demonstrated a deuterium isotope effect for [^{11}C]L-deprenyl trapping in the human brain. More specif-

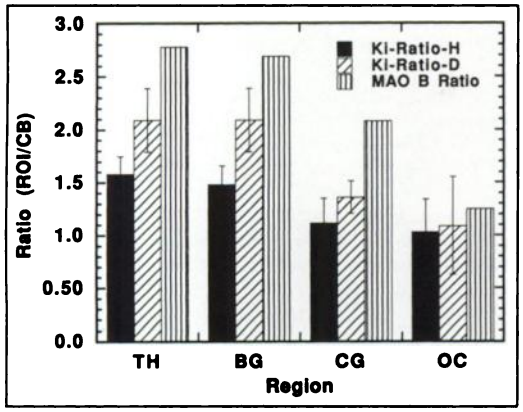

FIGURE 8. A bar graph of the ratio of the mean values ± s.d. of K_i for the ROI-to-cerebellum (CB) ratio, along with the same ratio for MAO B concentration from postmortem brain. The value for the cerebellum was taken from Glover et al. (*35*) and scaled to the other brain regions. Both tracers, [^{11}C]L-deprenyl (H) and [^{11}C]L-deprenyl-D2 (D) are presented. There is a greater range of values for [^{11}C]L-deprenyl-D2.

ically, we have shown that MAO B catalyzed cleavage of the carbon-hydrogen bond in the methylene carbon atom of the propargyl group of L-deprenyl contributes to the rate-limiting step for trapping of ^{11}C in tissue. We have also shown that deuterium substitution of the carbon-hydrogen bonds which are cleaved by MAO B does not affect K_1, but that it selectively reduces ^{11}C uptake in all brain regions as well as model terms related to the trapping of tracer in tissue. This study links the model terms K_i and $\lambda k'_3 E$ directly to MAO B concentration in the brain. This comparative study forms the framework for using [^{11}C]L-deprenyl-D2 to map human brain MAO B with enhanced sensitivity by allowing the separation of processes related to radiotracer delivery from processes related to radiotracer trapping. This significantly improves the assessment of regional human brain MAO B permitting these measurements in normal aging and in neurological and psychiatric disorders. This in vivo methodology will be useful to directly investigate in the living human brain many of the hypotheses from postmortem data and platelet MAO B analysis which suggests an association between MAO B and disease (*36*). Moreover, the association of MAO B with glial cells (*37,38*), provides an opportunity to track gliosis associated with normal aging and neurodegenerative processes and to monitor neuroprotective therapy. In fact, [^{11}C]L-deprenyl-D2 has been recently used successfully as a positive marker in the visualization of temporal lobe epilepsy with PET (Bergstrom M, et al. *unpublished data*.)

ACKNOWLEDGMENTS

The authors thank the United States Department of Energy (Office of Health and Environmental Research, Contract DE-AC02-76CH00016) and the National Institutes of Health (NS 15380 and NS 15638) for financial support; Donald Warner, Thomas Martin, Colleen Shea, Darrin Jenkins, Robert Carciello and Clarence Barrett for PET and Cyclotron operations and radiotracer synthesis; and Carol Redvanly for organizational assistance.

REFERENCES

1. Fowler CJ, Oreland L, Callingham BA. The acetylenic monoamine oxidase inhibitors clorgyline, deprenyl, pargyline and J-508: their properties and applications. *J Pharm Pharmacol* 1981;33:341–347.
2. Riederer P, Konradi C, Schay V. Localization of MAO-A and MAO-B in human brain: a step in understanding the therapeutic action of L-deprenyl. Yahr MD, Bergmann KJ, eds. *Advances in neurology*. New York: Raven Press; 1986:111–118.
3. Jossan SS, Gillberg P-G, Gottfries CG, Karlsson I, Oreland L. Monoamine oxidase B in brains from patients with Alzheimer's disease: a biochemical and autoradiographical study. *Neuroscience* 1991;45:1–12.
4. Jossan SS, Hiraga Y, Oreland L. The cholinergic neurotoxin ethylcholine mustard aziridinium (AF64A) induces an increase in MAO B activity in rat brain. *Brain Res* 1989;476:291–297.
5. Aquilonius S-M, Jossan SS, Ekblom JG, Askmark H, Gillberg P-G. Increased binding of 3H-L-deprenyl in spinal cords from patients with amyotrophic lateral sclerosis as demonstrated by autoradiography. *J Neural Transm* 1992;89:111–122.
6. Mann JJ, Petito A, Stanley M, McBride PA, Chin J, Philogene A. Amine receptor binding and MAO activity in postmortem human brain tissue; effect of age, gender and postmortem delay. *Biol Psychiatry New Prospects* 1985;5:37–39.
7. Strolin Benedetti M, Dostert P. Monoamine oxidase, brain ageing and degenerative diseases. *Biochem Pharmacol* 1989;38:555–561.
8. Oreland L. Monoamine oxidase, dopamine and Parkinson's disease. *Acta Neurol Scand* 1991;84(suppl):60–65.
9. Fowler JS, MacGregor RR, Wolf AP, et al. Mapping human brain monoamine oxidase A and B with ^{11}C-suicide inactivators and positron emission tomography. *Science* 1987;235:481–485.
10. Fowler JS, Wolf AP, MacGregor RR. Mechanistic positron emission tomography studies. Demonstration of a deuterium isotope effect in the MAO catalyzed binding of [^{11}C]L-deprenyl in living baboon brain. *J Neurochem* 1988;51:1524–1534.
11. Fowler JS, Volkow ND, Logan J, et al. Monoamine oxidase B (MAO B) inhibitor therapy in Parkinson's disease: the degree and reversibility of human brain MAO B inhibition by Ro 19-6327. *Neurology* 1993;43:1984–1992.
12. Bench CJ, Price GW, Lammerstma AA, et al. Measurement of human cerebral monoamine oxidase type B (MAO-B) activity with positron emission tomography: a dose ranging study with the reversible inhibitor Ro 19-6327. *Eur J Clin Pharmacol* 1991;10:169–173.
13. Fowler JS, Volkow ND, Logan J, et al. Slow recovery of human brain MAO B after L-deprenyl withdrawal. *Synapse* 1994;18:86–93.
14. Brust P, Riis Andersen PR, Diksic M, Gjedde A. Monoamine oxidase B activity in human brain measured with [^{11}C]L-deprenyl [Abstract] *J Cereb Blood Flow Metab* 1991;11:S227.
15. Arnett CD, Fowler JS, MacGregor RR, et al. Turnover of brain monoamine oxidase measured in vivo by positron emission tomography using L-[^{11}C]deprenyl. *J Neurochem* 1987;49:522–527.
16. Bench CJ, Lammertsma AA, Dolan RJ, Brooks DJ, Frackowiak RSJ. Cerebral monoamine oxidase B (MAO-B) activity in normal subjects, Alzheimer's disease and Parkinson's disease [Abstract]. *J Cereb Blood Flow Metab* 1993;13(suppl):S246.
17. Kim H-J, Zeeberg B, Reba R. Theoretical investigation of the estimation of relative regional neuroreceptor concentration from a single SPECT or PET image. *IEEE Trans Med Imaging* 1990;9:247–261.
18. Fenstermacher JD, Patlak CS, Blasberg RG. A new method for estimating plasma to tissue transfer constants. *Fed Proc* 1979;38:1138.
19. Patlak CS, Fenstermacher JD, Blasberg RG. Graphical evaluation of blood-to-brain transfer constants from multiple time-activity data. *J Cereb Blood Flow Metab* 1983;3:1–7.
20. Patlak CS, Blasberg RG. Graphical evaluation of blood-to-brain transfer constants from multiple time-activity data. Generalizations. *J Cereb Blood Flow Metab* 1985;5:584–590.
21. Gjedde A. High- and low-affinity transport of D-glucose from blood to brain. *J Neurochem* 1981;36:1463–1471.
22. Kearfott KJ, Rottenberg DA, Knowles RJR. A new headholder for PET, CT, and NMR imaging. *J Comput Assist Tomogr* 1984;8:1217–1220.
23. MacGregor RR, Fowler JS, Wolf AP. Synthesis of suicide inhibitors of monoamine oxidase: carbon-11 labeled clorgyline, L-deprenyl and D-deprenyl. *J Label Cmpds Radiopharm* 1988;25:1–9.

24. Matsui T, Hirano A. *An atlas of the human brain for computerized tomography*. Stuttgart: Gustav Fischer, 1978.
25. Shampine LF, Gordon MK. *Computer solution of ordinary differential equations: the initial value problem*. San Francisco: W.H. Freeman; 1975: 289–293.
26. Press WH, Flannery BP, Teukolsky SA, Vetterling WT. *Numerical recipes. The art of scientific computing*. Cambridge: Cambridge University Press; 1986.
27. Logan J, Dewey SL, Wolf AP, et al. Effects of endogenous dopamine on measures of [^{18}F]N-methylspiroperiodl binding in the basal ganglia: comparison of simulations and experimental results from PET studies in baboons. *Synapse* 1991;9:195–207.
28. Melander L, Saunders WH Jr. *Reaction rates of isotopic molecules*. New York: John Wiley and Sons; 1980.
29. Belleau B, Moran J. Deuterium isotope effects in relation to the chemical mechanism of monoamine oxidase. *Ann NY Acad Sci* 1963;107:822–839.
30. Hashimoto K, Inoue O, Suzuki K, Yamasaki T, Kojima M. Deuterium isotope effect of [^{11}C]N,N-dimethylphenethylamine-α,α-d2; reduction of the metabolic trapping rate in brain. *Nucl Med Biol* 1986;13:79–80.
31. Tominaga T, Inoue O, Suzuki K, Yamasaki T, Hirobe M. [^{13}N]-β-phenethylamine ([^{13}N]PEA): a prototype tracer for measurement of MAO-B activity in heart. *Biochem Pharmacol* 1987;36:3671–3675.
32. Walsh C. Suicide substrates: mechanism based enzyme inactivators. *Tetrahedron* 1982;38:871–909.
33. Oreland L, Arai Y, Stenstrom A, Fowler CJ. Monoamine oxidase activity and localisation in the brain and the activity in relation to psychiatric disorders. *Mod Probl Pharmacopsychiat* 1983;19:246–254.
34. Fowler CJ, Wiberg A, Oreland L, Marcusson J, Winblad B. The effect of age on the activity and molecular properties of human brain monoamine oxidase. *J Neural Transm* 1980;49:1–20.
35. Glover V, Elsworth JD, Sandler M. Dopamine oxidation and its inhibition by (−)-deprenyl in man. *J Neural Transm* 1980;16(suppl):163–172.
36. Fowler CJ, Tipton KF, McKay AVP, Youdim MBH. Human platelet monoamine oxidase—a useful enzyme in the study of psychiatric disorders. *Neuroscience* 1982;7:755–759.
37. Levitt P, Pintar JE, Breakefield XO. Immunocytochemical demonstration of monoamine oxidase B in brain astrocytes and serotonergic neurons. *Proc Natl Acad Sci USA* 1982;79:6385–6389.
38. Ekblom J, Bergstrom M, Oreland L, Walum W, Aquilonius S-M. Monoamine oxidase B in astrocytes. *Glia* 1993;8:122–132.